Appl Intell (2018) 48:1368–1378
DOI 10.1007/s10489-017-1042-9

# A novel three-band orthogonal wavelet filter bank method for an automated identification of alcoholic EEG signals

**Manish Sharma[1] · Dipankar Deb[1] · U. Rajendra Acharya[2,3,4]**

Published online: 17 August 2017


**Abstract** Alcoholism is a critical disorder related to the central nervous system, caused due to repeated and excessive consumption of alcohol. The electroencephalogram (EEG) signals are used to depict brain activities. It can also be employed for diagnosis of subjects consuming excessive alcohol. In this study, we have developed an automated system for the classification of alcoholic and normal EEG signals using a recently designed duration-bandwidth product (DBP), optimized three-band orthogonal wavelet filter bank (TBOWFB), and log-energy (LE). First, we obtain sub-bands (SBs) of EEG signals using the TBOWFB. Then, we use logarithms of the energies of the SBs as the discriminating features which are fed to the least square support vector machine (LS-SVM) for the discrimination of normal and alcoholic EEG signals. We have achieved a classification accuracy (CA) of 97.08%, with ten-fold cross validation strategy. The proposed model presents a promising performance, and therefore it can be used in a practical setup to assist the medical professionals in the diagnosis of alcoholism using EEG signals automatically.

✉ Manish Sharma
manishsharma.iitb@gmail.com

[1] Department of Electrical Engineering, Institute of Infrastructure, Technology, Research and Management (IITRAM), Ahmedabad, 380026, India

[2] Nagee Department of Electronics and Computer Engineering, Ngee Ann Polytechnic, Singapore 599489, Singapore

[3] Department of Biomedical Engineering, School of Science and Technology, SUSS University, Singapore, Singapore

[4] Department of Biomedical Engineering, Faculty of Engineering, University of Malaya, Malaya, Malaysia

**Keywords** Alcoholism · Electroencephalogram (EEG) · Optimal three-band filter banks · Duration-bandwidth product · Wavelets

## 1 Introduction

Alcoholism is regarded as a serious and specialized kind of psychoactive substance abuse disorder which mainly depends on the consumption and pattern of drinking. Studies of World Health Organization (WHO) reveal that an approximate number of 3.3 million deaths each year have been caused due to alcohol usage, accounting for close to 5.9% of all deaths worldwide. Approximately 2 billion people consume alcohol in different forms and of those, 81.7 million are serious addicts whose alcohol dependency is characterized by symptoms that can be diagnosed. Moreover, alcohol dependency considerably increases disability-adjusted life-years (DALY) and as per estimates, 139 million DALYs, or 5.1% of net diseases and injuries worldwide, are directly attributable to intake of alcohol [11, 29]. Additionally, increasing occurrence of cancers related to alcohol further highlights this serious concern [16]. These adverse effects accentuate the need for advanced research aimed at cost-effective and early diagnosis and monitoring of alcohol abuse [19].

Electroencephalography (EEG) is a non-invasive physiological test that provides brain signals for analysis of neuropsychiatric states. In the absence of a detailed brain model describing complete functionalities, researchers are dependent on empirical methods which suggest the non-linear and non-stationary behavior of EEG signals. The non-linearity makes the analysis of EEG signals a challenging task [28]. Machine learning and signal processing based techniques that process psychological signals are used to

extract significant features which are then fed as input to classification algorithms [18]. It is desirable to choose a fast and reliable method for extraction of features and the consequent classification. Towards achieving this objective, many machine learning and signal processing based methods have been explored for the analysis and classification of various subgroups of EEG signals [3, 6, 8, 34, 38]. In particular, several automated systems have been developed to identify the alcoholic state of subjects [1, 3, 20, 30]. Ehlers et al. [17] studied the nonlinear brain dynamics using chaos theory as applied to EEG signals obtained from 32 individuals. For feature extraction, correlation dimension (CD) was used along with discriminant analysis. Kannathal et al. [25] have used chaotic measures such as Lyapunov exponent (LLE), Hurst exponent (HE) CD, largest , and some entropy based features to characterize the signal and to obtain diagnostic features for the characterization of alcoholism from EEG signals. Results indicated that these nonlinear measures were good discriminators of normal and alcoholic EEG signals.

Acharya et al. [3] have proposed a computer aided diagnostic (CAD) technique for the automated identification of non-alcoholic and alcoholic EEG signals using nonlinear features such as approximate entropy (APPENT), LLE and higher order spectra (HOS). The SVM was used to separate normal and alcoholic signals. Faust et al. [20] have presented a processing system which classifies EEG signals into alcoholic and non-alcoholic classes. The identification system is done using wavelet packet transform (WPT), which decompose EEG signals into various subbands (SBs), and energy measures. More recently, Patidar et al. [30] have proposed a new alcoholism diagnosis scheme using Tunable-Q Wavelet Transform (TQWT) and Correntropy (CE) based feature extraction. These features are then fed LS-SVM classifier which has led to promising classification performance. Two-band wavelet filter banks (FBs) have been extensively used for analysis of EEG signals [8, 34, 38, 40]. However, the analysis using two-band FBs suffers from poor frequency resolution in low and high frequency bands. Recently, in few studies [6, 7], time-frequency localized three-band wavelet filter banks have been used for the classification of various classes of EEG signals. The time-frequency localized three-band filter banks have shown excellent performance in discriminating seizure and seizure-free classes of EEG signals [6]. It is also conjectured by Bhati et al. [6] that the two-band filter banks extract features with poorer discrimination ability than the optimal three band wavelet filter banks. The joint time-frequency localization of filters and bases play an important role in the analysis and processing of non-stationary signals. The bases with minimum joint localization are highly desirable. However, uncertainty poses a lower bound on time-bandwidth localization. Due to this, it is not possible to arbitrarily localize a signal in time and frequency at the same time. The time-bandwidth optimized three band orthogonal wavelet filter banks (TBOWFBs) have been found very useful in the analysis of non-stationary signals including EEG Signals [34]. TBOWFB have been proven to be effective in edge detection, image compression, image segmentation, image enhancement and feature extraction [32–34]. However, the performance of three band wavelet FBs has yet not been evaluated in classifying alcoholic and normal EEG signals. This motivated us to develop an automated system for the identification of alcoholic state using the three band wavelet FBs. In this study, we have developed a CAD that uses duration-bandwidth product (DBP) optimized three-band orthogonal wavelet filter bank (TBOWFB) to decompose EEG signals into 7 SBs obtained through three levels of decomposition. Then log of energy (LE) of each of the 7 SBs have been computed. The student's t-test is used to measure the discriminating ability of each feature. The LEs feature-vector is then applied to the LS-SVM classifier to distinguish normal and alcoholic signals. The 10-fold cross-validation (CV) has been used and classification performance of the proposed model has been expressed in terms of CA, classification sensitivity (CE) and classification specificity (CSF).

## 2 Materials and method

The flow of the process to develop the proposed system is depicted in Fig. 1. The first step is to acquire EEG data to be analyzed, which is followed by the pre-processing (filtering) of the raw EEG data to remove unwanted artifacts. The processed EEG signals thus obtained are decomposed into various SBs. For the SB decomposition of the EEG signals, a new class of optimal DBP localized TBOWFB is employed in this work. Having obtained SBs of the signals the next step is to calculate LEs of each SB. The (LEs) are used as discriminating features. The feature vector set comprises 7 LE features ranked using student's t-test and then applied to the LS-SVM classifier.


**Fig. 1** Block diagram of the proposed model

**Table 1** Details of EEG dataset for alcoholic and normal subjects

| Class of Subjects | Number of segments | Sampling Frequency | Number of samples |
|---|---|---|---|
| Alcoholic | 120 | 256 Hz | 2048 |
| Normal | 120 | 256 Hz | 2048 |

### 2.1 Data acquisition and prepossessing

The EEG dataset employed in the proposed study is acquired from University of California, Irvine knowledge discovery in database http://kdd.ics.uci.edu/databases/eeg/eeg.data.html. This dataset was collected during a large study which examined the correlation of EEG with a predisposition to alcoholism. The dataset includes the EEG recordings acquired from entire 10/20 international montage or standard sites. Each of the subjects involved has undergone 120 trials for different stimuli consisting of 90 images. These EEG signals also contain event-related bio-potentials obtained by 64 electrodes placed on the scalp. Subjects were grounded with a nose electrode with the impedance less than 5 k ohm. Two additional bipolar deviations were used to record vertical and horizontal electrooculography (EOG). The signals were sampled at a frequency of 256 Hz for 32 s. Trials with high eye and body movements ($> 73.3\mu$V) were discarded and then 30 EEG recordings for non-alcoholic and 30 recordings for the alcoholic group were obtained. These recordings were then split into four parts of 8 seconds (each segment containing 2,048 samples). Thus, 120 data segments each for subjects denoted as normal and alcoholic were obtained. Important information related to the data is summarized in Table 1. Figure 2 shows sample data segments corresponding to normal and alcoholic subjects. Figure 3 depicts the spectra of sample data segments shown in Fig. 2.

### 2.2 Design of optimal DBP localized TBOWFB and SB decomposition

In this study, we have used a new class of optimal DBP localized TBOWFBs to analyze EEG signals [7]. A typical three-band filter bank is shown in Fig. 4. The analysis bank comprises three filters namely, analysis lowpass filter (ALF) $H_0(z)$, analysis bandpass filter (ABF) $H_1(z)$ and analysis highpass filter (AHF) $H_2(z)$. Similarly, the synthesis banks are also composed of three filters namely synthesis lowpass filter (SLF) $F_0(z)$, synthesis bandpass filter (SBF) $F_1(z)$ and synthesis highpass filter (SHF) $F_2(z)$. In two-band filter bank [39], the sequence is downsampled and upsampled by a factor of 2 but in the case of a three-band filter bank the sequence is down and up sampled by a factor of 3. The cascade iterations [47] of TBOWFB generate one scaling function $\phi(t)$ and two wavelet functions $\psi_1(t)$ & $\psi_2(t)$ unlike Daubechies two-band orthogonal filter banks [15], which yield one scaling function $\phi(t)$ and one wavelet function $\psi_1(t)$. Wavelets are often designed through iterations of two-band filter banks [47], but those constructed from three-band filter banks possess some desirable features such as increased control on time-frequency tiling and fine analysis of narrow-band high-frequency signals [10]. Additionally, TBOWFBs also offer linear phase and orthogonality together, which is not possible with two-band Filter banks (FB) [12]. It is possible to generate three-band orthogonal wavelets from the regular three-band para unitary FBs [22]. The regularity or equivalently vanishing moments (VMs) and orthogonality conditions can be structurally imposed using the technique given by Vaidyanathan et al. [45, 46]. Recently, design of three band FBs has received a lot of attention from many researchers. Multiple methodologies for the design of three-band FBs have been proposed in the literature. Many authors [7, 12, 24, 27, 31, 49] have developed TBOWFBs and [23, 41] have suggested techniques to design three-band biorthogonal wavelet FBs. In this study,

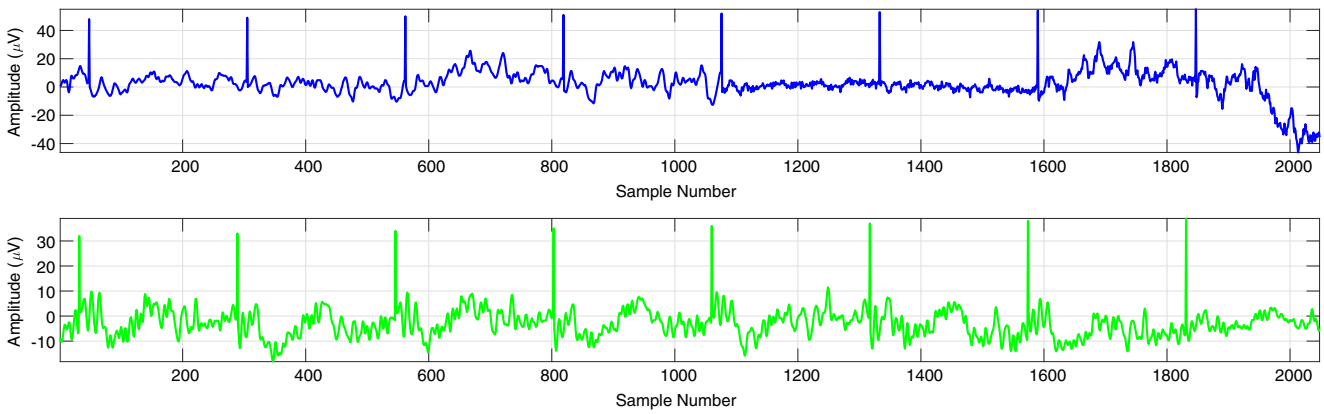


**Fig. 2** *Top*: normal EEG signal segment, *bottom*: alcoholic EEG signal segment

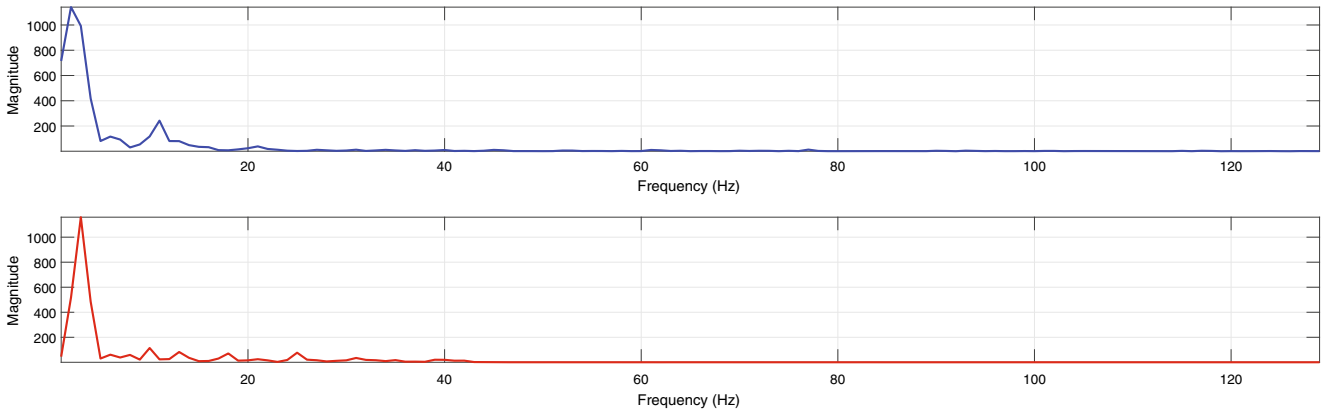


**Fig. 3** *Top*: Spectrum of normal EEG segment, *bottom*: spectrum of alcoholic EEG segment

we utilize dyadic factorization of polyphase matrix formulation given by Vaidyanathan [45, 46] to construct orthogonal three-band filter bank. The filter bank (FB) design problem has been cast as a constrained optimization problem wherein the objective function is a weighted combination of duration-bandwidth product(DBP) [35] of the scaling function $\phi(t)$ and wavelet functions $\psi_1(t)$ & $\psi_2(t)$. The time spread and frequency spreads of a scaling function or wavelets are measured as second order moments of the signal and its Fourier transform, respectively [21, 36]. The product of these moments (variances) is referred to as duration-bandwidth product (DBP) of the function [34]. According to Gabor's uncertainty principle, the DBP of a function is lower bounded by 0.25 [21]. The scaling and wavelet functions generated through the cascade iterations [48] of the optimal TBOWFB posses DBP close to the lower limit. The DBP optimized wavelet FBs are found to be very useful in the analysis of non-stationary, transient and bio-signals including EEG signals [32, 33, 36, 37, 40].

For a three-band filter bank, the analysis scaling function $\phi(t)$ and analysis wavelet functions $\psi_1(t)$ and $\psi_2(t)$ can be derived from the three analysis filters as given below [45, 46]:

$$\phi(t) = \sqrt{3}\sum_n h_0[n]\phi(3t-n) \tag{1}$$

$$\psi_1(t) = \sqrt{3}\sum_n h_1[n]\phi(3t-n) \tag{2}$$

$$\psi_1(t) = \sqrt{3}\sum_n h_2[n]\phi(3t-n) \tag{3}$$

In this study, the cascade algorithm [48] has been used to construct scaling and wavelet functions from the iterations of the filters.

### 2.3 Duration bandwidth localization

Let $g(t)$ be a continuous-time real valued function in $L_2(\mathbb{R})$. Let $G(\omega)$ be its Fourier transform. The time spread can be calculated in terms of time variance $\sigma_t^2$ of the function, given as follows [21]:

$$\sigma_t^2 = \frac{1}{\|g(t)\|^2}\int_{t\in\mathbb{R}}(t-t_0)^2|g(t)|^2dt \tag{4}$$

where, the time mean $t_0$ can be given as

$$t_0 = \frac{1}{\|g(t)\|^2}\int_{t\in\mathbb{R}} t|g(t)|^2dt \tag{5}$$

The time variance $\sigma_t^2$ is referred to as duration of the function $g(t)$. The frequency spread of a function in $L_2(\mathbb{R})$ can be measured in terms of frequency variance defined as below [21]:

$$\sigma_\omega^2 = \frac{1}{2\pi\|G(\omega\|^2}\int_{\omega\in\mathbb{R}}(\omega-\omega_0)^2|G(\omega)|^2d\omega \tag{6}$$

where frequency mean $\omega_0$ is given as:

$$\omega_0 = \frac{1}{2\pi\|G(\omega\|^2}\int_{\omega\in\mathbb{R}}\omega|G(\omega)|^2d\omega \tag{7}$$

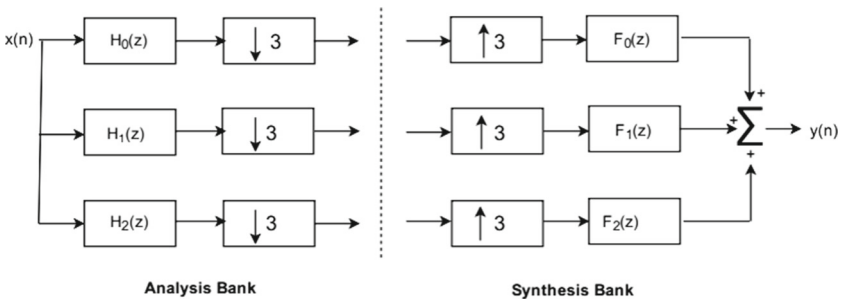


**Fig. 4** Typical three-band filter bank

The frequency variance is referred to as bandwidth of the function. The Gabor's uncertainty principle [21] poses the restriction that continuous-time function cannot be arbitrarily localized in both domains simultaneously. In particular, the product of bandwidth and duration, as defined in (4) and (6), of the signal $g(t) \in L_2(\mathbb{R})$ is lower bounded as given by the following inequality:

$$\Delta_g = \sigma_t^2 \, \sigma_\omega^2 \geq \frac{1}{4}, \tag{8}$$

The $\Delta_g$ is called DBP of the signal $g(t)$.

### 2.4 Optimization method

Our objective is to obtain optimal three-band scaling and wavelet filters that yield wavelet bases $\{\phi(t), \psi_1(t), \psi_2(t)\}$ with minimum DBP. We minimize the following objective function:

$$\Phi = \alpha\Delta_\phi + \beta\Delta_{\psi_1} + \gamma\Delta_{\psi_2}, \alpha, \beta, \gamma \geq 0, \alpha+\beta+\gamma = 1 \tag{9}$$

where $\Delta_\phi$, $\Delta_{\psi_1}$and $\Delta_{\psi_2}$ are DBPs of the scaling and wavelets functions, respectively. $\alpha, \beta, \gamma$ are weight factors for controlling DBP of scaling and wavelet functions. The filters of a underlying TBOWFB should satisfy the constraints of triple-shift orthogonality and VMs [6, 45, 46]. Thus, the filter bank design problem can be formulated as the following constrained optimization problem:

$$\begin{aligned} &\underset{[h_0(n),h_1(n),h_2(n)]}{\text{minimize}} \quad \Phi \\ &\text{subject to} \quad < h_l[-n], h_m[n-3p] > \\ &\qquad\qquad = \delta(l-m)\delta(p)l, m = 0, 1, 2 \\ &\qquad\qquad H_0(e^{j2\pi/3}) = H_0(e^{j4\pi/3}) = 0 \end{aligned} \tag{10}$$

where $H(e^{j\omega})$ denotes the discrete-time Fourier transform (DTFT) of the filter $h(n)$ given as

$$H(e^{j\omega}) = \sum_{n\in\mathbb{Z}} h(n)e^{-j\omega n} \tag{11}$$

The solution for the above constrained optimization problem (10) gives rise to three optimal filters $h_0(n)$, $h_1(n)$ and $h_2(n)$. The cascade iteration of these optimal filters yield optimal scaling function $\phi(t)$ and two optimal wavelet functions $\psi_1(t)$ & $\psi_2(t)$. The weighted combination of DBPs of these optimal scaling and wavelet functions has the minimum value. The limitation of the above optimization problem (10) is that number of free variables are directly proportional to the lengths of the filters to be designed. As the lengths of the filters increase the number of optimization variables increase linearly. Thus for higher order filters, the optimization algorithm used to obtain the variables may yield non-optimal or suboptimal solution. In order to have filter design techniques where the number of unknown variables does not increase linearly with filter-length, the parametrization based approaches [45, 46] can be used. In this study, we use the paraunitary structure given by Vaidyanathan [45, 46] with fewer free variables to design the filters wherein orthogonality and regularity conditions are imposed in the structure itself. Using the parametrization technique, we have transformed the optimization problem (10) in the unconstrained optimization problem (12) wherein the conditions of orthogonality and VMs are imposed structurally. This facilitates us in reducing the space of search and it also avoids imposing constraints.

$$(h_0^*(n), h_1^*(n), h_2^*(n)) = \arg\min_{\{\theta_i\}}(\Phi(\theta_i)) \tag{12}$$

The $\{\theta_i\}$ represents the set of free parameters and $((h_0^*(n), h_1^*(n), h_2^*(n))$ are the optimal filter coefficients. The whole optimization procedure can be summarized in the following steps:

1. Choose the desired lengths and VMs for the filters. Employ Vaidyanathan's [31, 45] parametric technique to design filters.
2. Formulate the unconstrained optimization problem given in (12), select appropriate initial values for the free parameters $\{\theta_i\}$.
3. Perform the optimization using Matlab's optimization toolbox with objective function $\Phi$ as given in (9) to obtain the set of optimal parameters $\{\theta_i\}$
4. Store the values of optimal free parameters corresponding to the minimum value of the objective function. Generate the optimal filter coefficients using the stored optimal free parameters.

The optimal filters thus obtained have been used in the proposed automated system for the classification of alcoholic and normal signals. We employ three-level of wavelet decomposition that yield total 7 SBs for each input EEG signals. Thereby, using the proposed TBOWFB, each EEG signal has been decomposed into 7 SBs occupying different spectral regions (frequencies).

#### *2.4.1 A design example*

To illustrate the effectiveness of the design method for optimal DBP localized TBOWFB, we present a design example that generates the optimal scaling and wavelet filters.

*Example:* In this example, we design three band orthogonal wavelet filters each of length six. The order of the regularity is chosen to be one. For the optimization problem (12), we choose the weight factors as $\alpha = 0$, $\beta = 1$, $\gamma = 0$. The solution for optimization problem yields three optimal filters. The impulse responses of the filters are shown in Fig. 5. The pole-zero plots of optimal filters are shown in Fig. 6. In complex z-plane, the locations of zeros give the frequencies at which the amplitude response of the filter vanishes. Similarly, the location of zeros gives

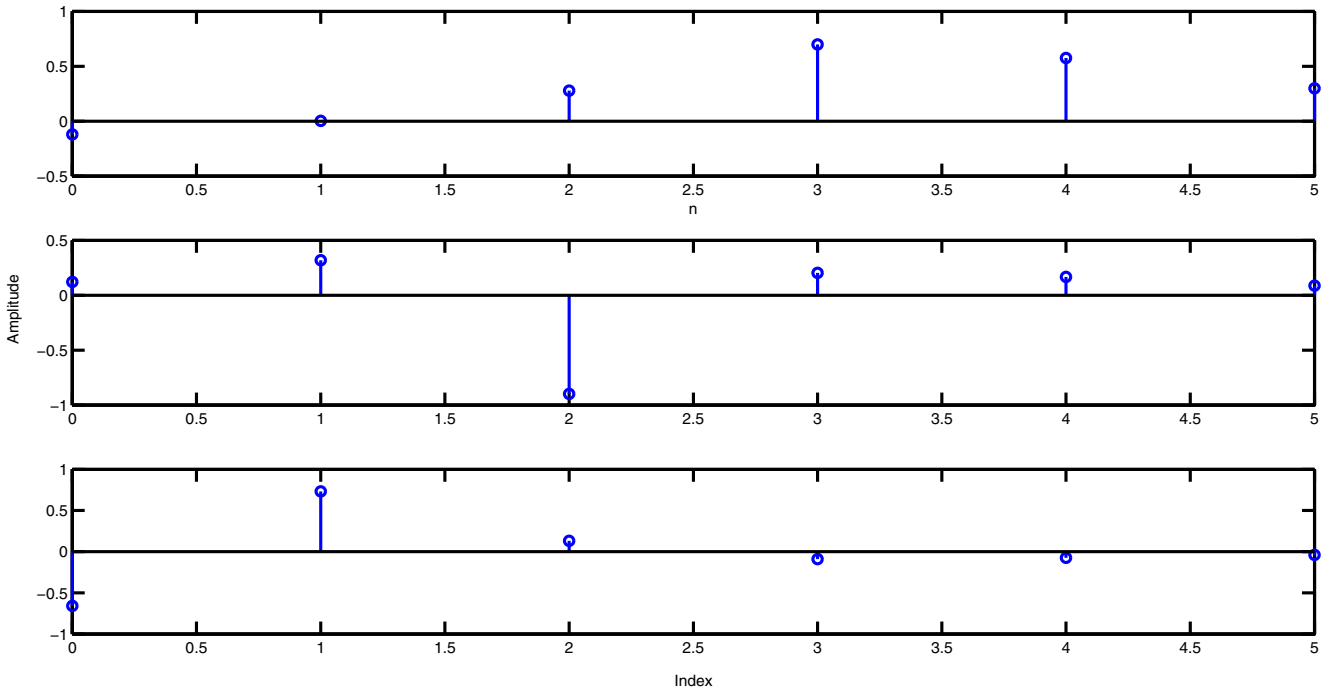


**Fig. 5** Impulse responses of length-six optimal scaling and wavelet filters, *top*:ALF, *middle*:BPF, *bottom*:AHF

the frequencies at which the response tends towards infinity. The pole-zero plots have been drawn to show that the filters of underlying FB satisfy the regularity condition. A 3-band orthogonal FB is said to be K-regular if the LPF has frequency $\omega = (2m\pi/3)$, where $m = 1, 2$. And, other filters have $k$ zeros at frequency $\omega = 0$. From Fig. 6, it

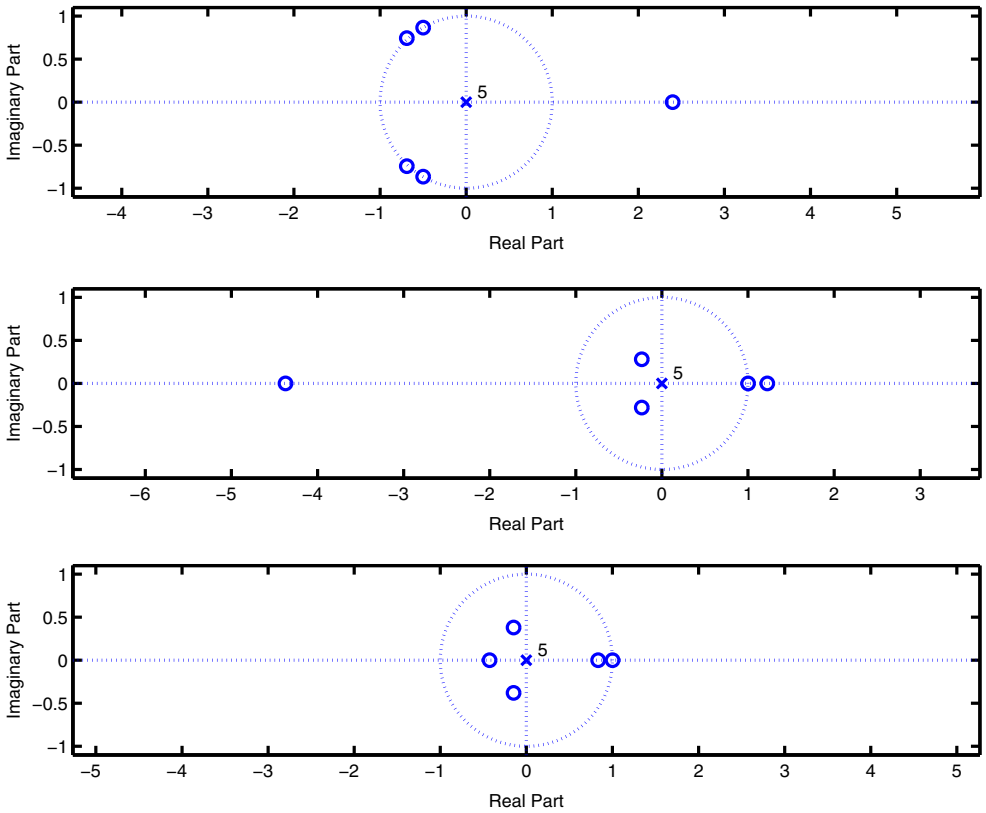


**Fig. 6** Pole-zero plots of optimal filters, *top*:ALF, *middle*:BPF, *bottom*:AHF

is clear that the lowpass filter has zeros at frequency $2\pi/3$ and $4\pi/3$. And, both bandpass and highpass filters have a zero at $\omega = 0$. Thus the filter bank considered in the example is 1-regular. In other words the order of regularity index is one. The value of the cost function obtained is 3.238. The wavelets and scaling functions are generated through 8 iterations of the optimal filters. Figure 7 shows the plots of generated wavelets and scaling functions. The DPB of the scaling function $\phi(t)$ designed from the optimal filters is 1.0260 whereas for optimal wavelet functions $\psi_1(t)$ and $\psi_1(t)$, the DPBs are 3.2384 and 3.6009, respectively.

### 2.5 Feature extraction and ranking

Having obtained 7 wavelet SBs, we compute the logarithm of energy (LE) for all seven SBs for each EEG signals. We use these wavelet based LEs as the discriminating features to classify normal and alcoholic EEG signals.
Let $x(n)$ be wavelet time series corresponding to a SB of a EEG signal. The LE of the sequence $x(n)$ has been defined as

$$x_{LE} = \ln \sum_{n \in \mathbb{Z}} |x(n)|^2 \tag{13}$$

Besides, feature ranking is done in order to test the statistical significance of each of 7 LE features. For feature ranking, student's t-test [50] is used and then the features are ranked in order of t-values. p-values are also computed corresponding to each feature using the t-test.

### 2.6 Classification and cross validation

Recently, the usage of support vector machines (SVM) that employ supervised learning model for classification and regression analysis, and originally developed by Vapnik et al. [13, 44], has been widespread. Boser et al. [9] and Cristianini et al. [9, 14] have formulated kernel-based SVMs. An improved variant of SVM, the least squares support vector machines (LS-SVM) classifiers developed by Suykens et al. [42], have proved to be efficient in accurately classifying biomedical signals including EEG signals [34], and received much attention from machine learning researchers. In this technique, the classification error is minimized by data mapping into a higher dimensional space and by construction of an optimal separating hyperplane with minimal distance from all of the classes.

In the proposed model, we employ quadratic and Gaussian Radial basis function (RBF) kernel. The RBF kernel is given by [34]

$$\mathbb{k}(\chi, \chi_m) = e^{\frac{-|\chi - \chi_m|^2}{2\sigma^2}} \tag{14}$$

where $\sigma^2$ is the variance of the kernel. For optimal performance, $\sigma$ is varied within the range 1 to 20 taking intervals of .1.

**Table 2** Results of t-test: ($\mu \pm \sigma$) represents the range (mean $\pm$ standard deviation) of normal and alcoholic features

| SB | Alcohol $\mu \pm \sigma$ | Normal $\mu \pm \sigma$ | p-value |
|---|---|---|---|
| 1 | 5.244±0.3630 | 5.9150±0.2094 | 1.007e-34 |
| 2 | 4.0157±0.4695 | 4.2441±0.3654 | 7.179e-26 |
| 3 | 4.0565±0.4310 | 4.2524±0.3430 | 4.100e-25 |
| 4 | 4.2945±0.2791 | 4.7200±0.2763 | 5.334e-22 |
| 5 | 4.2902±0.2785 | 4.7104±0.2781 | 8.084e-22 |
| 6 | 4.3676±0.2844 | 4.9429±0.3680 | 2.315e-04 |
| 7 | 4.3555±0.3093 | 4.9236±0.3506 | 9.208e-04 |

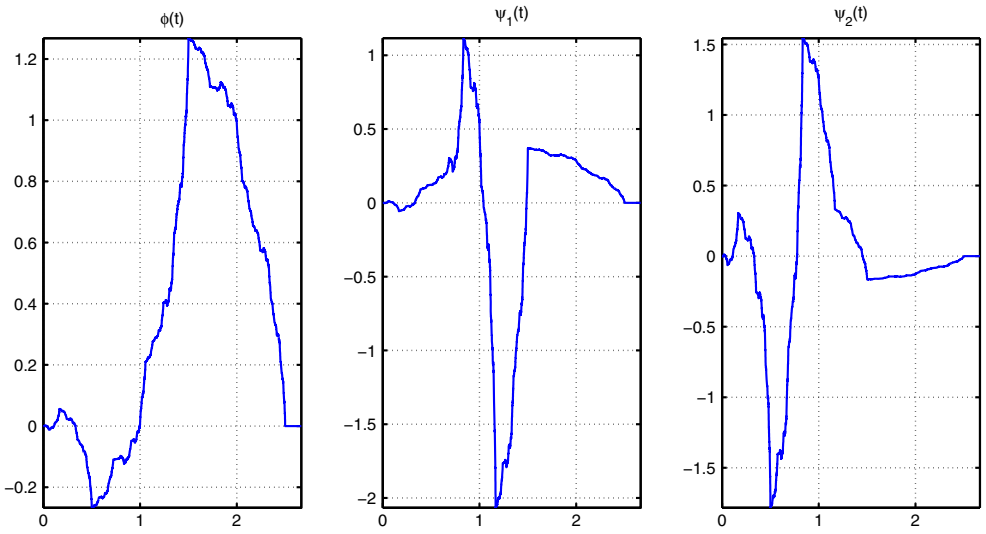


**Fig. 7** Scaling function and wavelets generated from DBP optimal TBOWFB

**Table 3** Classification performance of LS-SVM using RBF and quadratic Kernels

| Kernel | CA(%) | CS(%) | CSF(%) |
|---|---|---|---|
| RBF | 97.08 | 97.08 | 97.08 |
| Quadratic | 96.37 | 94.92 | 97.82 |

For reliable and robust performance sans over-fitting, we use 10-fold CV [26] wherein the data is segmented into ten mutually exclusive subsets, to evaluate the classification accuracy. Any one of the subsets is regarded as the testing subset whereas the remaining nine subsets are treated as the training subsets, and the process is iterated ten times with a different testing subset in each case, and the remaining subsets are the training subsets. The k-fold validation helps in minimizing the computational burden on the classifier and to mitigate information redundancy. The classification accuracy is measured for each iteration, and their average is computed.

## 3 Results and discussion

In Table 2, we present the results obtained from Student's t-test for all 7 LE features. From this table it is evident that all 7 features are clinically important and significant as the p-vales are very low ($p < 0.0001$). Further, in Fig. 8, we have shown the box plots for each of 7 LEs used in the classification process to verify if the LE values can differentiate normal and alcoholic EEG signals. From the figure, it is clear that LEs of normal and alcohol EEGs are mostly non-overlapping. The separation in the box plots is clearly significant. In fact, box plots corresponding to SB-1, SB-4, SB-6, SB-7 are completely separated which indicates very high discrimination ability of LEs corresponding to these SBs. Table 3 presents the classification results in terms of average CA, CS and CSF. For classifying LE features normal and alcoholic LS-SVM classifier is used with two different kernel functions namely RBF and quadratic kernel. From Table 3, it is clear that RBF kernel, with optimal value of $\sigma = 3$, performed better than quadratic kernel. The table indicates that the proposed model attained the highest CA of 97.08%. Figure 9 shows the CA for each fold of 10-fold CV strategy.

Table 4 compares the performance of our CAD system with the existing alcoholic identification systems using EEG signals. The entries in the table are arranged in order of the year of publication (YoP) of the work; proposed work is indicated in the last row of the table. The table indicates that our proposed model surpasses all the other existing models in terms of CA. It can be understood from the table that few researchers [17, 25, 43] have used linear models for the analysis of EEG signals alcoholic and normal controls. However, in these techniques, they have not employed any classification algorithms. Therefore, in the table, the entries corresponding to the classification performance is indicated as not applicable (NA), for these methods [17, 25, 43].

Faust et al. [19, 20] classified alcoholic and normal signals by employing power spectral density (PSD) extraction methods. They found the area under the curve (AUC) of receivers operating characteristics(ROC) to be 0.8222. The

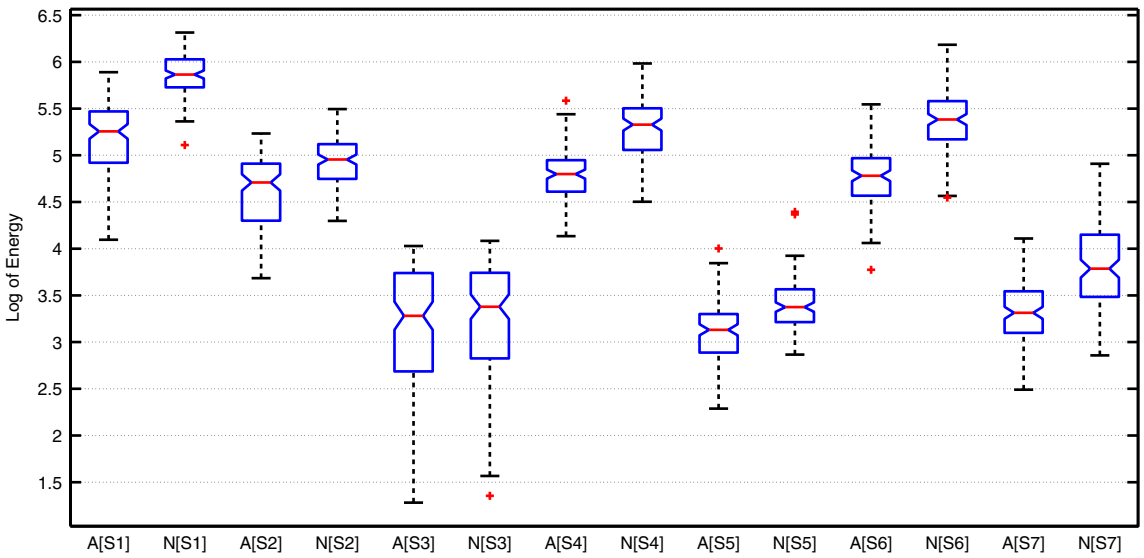


**Fig. 8** Boxplots for all 7 features: The notations $A[Si]$ and $N[Si]$ correspond to $i^{th}$ SB of alcohol and normal EEG signal

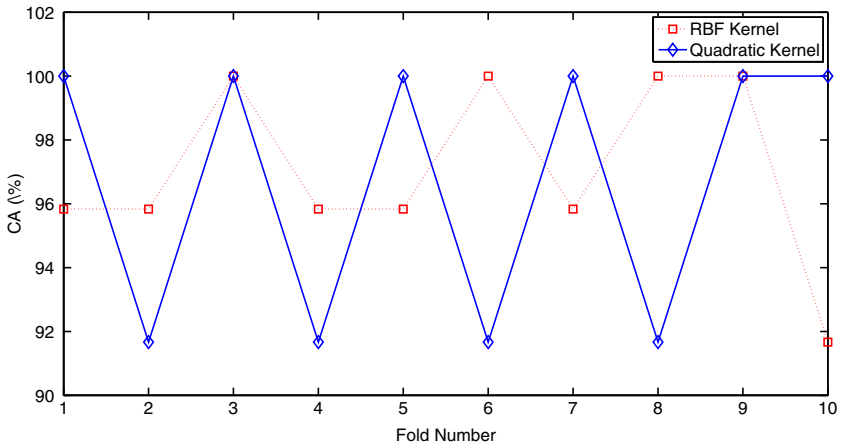


**Fig. 9** Variation of CA with respect to folds of 10-fold CV

authors have evaluated the performance only in terms of AUC-ROC, they have not mentioned the CA explicitly. In another work, Faust et al. [20] have developed an automated system using wavelet packet based energy measures and the k-nearest neighbor (KNN) classifier and achieved maximum CA of 95.8%. In this study, Faust et al. have used level-3 wavelet packet decomposition using Debaucheries orthogonal wavelet filter banks [15], level-3 wavelet packet decomposition yields a total of 16 SBs. It is noteworthy that we have used level-3 wavelet decomposition instead of wavelet packet decomposition, which generated 7 SBs only. For the given number of decomposition level, the computational cost of wavelet packet decomposition is higher than three-band wavelet decomposition. Moreover, our proposed model gives better classification performance than a model by Faust et al. [20] as we have attained a CA of 97.08%.

Acharya et al. [3] have employed non-linear features such as SAMENT, APPENT, LLE and HOS with LS-SVM classifier. They attained maximum CA of 91.7%. It is to be noted that computational cost of extracting the non-linear features used by Acharya et al. [3] is higher than the cost of LE feature used by us in this study. Further, the CA attained by our model is significantly higher than the model of Acharya et al. [3]. This is because features extracted from the SBs of EEG signals have better discrimination ability than the original EEG signals.

Recently Patidar et al. [30] have proposed an automated system for the diagnosis of alcoholism. They have employed Tunable Q-wavelet transform (TQWT) for wavelet decomposition of EEG signals. The authors have extracted CE of SBs obtained from TQWT. It is important to note that TQWT is a oversampled and highly redundant variant of wavelet transform whose computational complexity is

**Table 4** Comparison with existing methods using the same database

| Authors, YoP | Features/Methods | Classification Technique | Classification Performance |
|---|---|---|---|
| (Ehlers et al. [17], 1998) | CD, discriminant analysis | No classifier | NA |
| (Kannathal et al.[25], 2005) | CD, LLE, entropy | No classifier | NA |
| (Faust et al.[19], 2008) | PSD | ANN and SVM | 0.822 (AUC-ROC)) |
| (Tcheslavski & Gonen,[43], 2012) | Parametric spectral | No classifier | NA |
| | statistical analysis | | |
| | coherence measure | | |
| (Acharya et al.,[3], 2012) | APPENT, SAMENT, LLE, HOS | SVM | 91.3% (CA) |
| (Faust et al.[20], 2013) | WPT, energy measures | KNN | 95.8% (CA) |
| (Patidar and [30], 2017) | TQWT, CE | LS-SVM and | 97.02% (CA) |
| Our work | DBP Optimal TBOWFB and LE | LS-SVM | 97.08% (CA) |

higher than the critically sampled TBOWFB which is used by us in the proposed model. Further, the cost of computing non-linear CE is also higher than LE. The model of Patidar et al. [30] gave the highest CA of 97.02% which is comparable by our highest CA of 97.08% obtained from the proposed model.

The p-values of our features as given in Table 2 are significantly smaller than the p-values used by Faust et al. [20], Acharya et al. [3] as well as Patidar et al. [30] which indicates the better discriminating capability of our features. From Table 2, it is clear that all LE features are higher for normal as compared to alcoholic EEG signals. Hence, it is confirmed that alcoholic EEG signals are less random as compared to normal EEG signals [1, 3].

Further, it is to be noted that though t-test can be used as an indicator for evaluating discriminating ability of an individual feature, it cannot be used as a measure to gauge the collective discriminatory ability of all features when they are grouped to form a vector-feature. The classification algorithms along with the k-fold CV can be employed to measure the discriminating ability the vector-feature. From Table 4, it is evident that for the proposed model, LS-SVM classifier with RBF kernel in conjunction with 10-fold CV presents promising classification performance with CA, SE and CSF each of 97.08%.

## 4 Conclusion

We have developed a new computer-aided system for the diagnosis of alcoholism using EEG signals and DBP optimized TBOWFB. The LS-SVM classifier with RBF kernel and quadratic kernels have been used to separate normal and alcoholic EEG signals. To mitigate over-fitting and redundancy in the proposed model, we employed 10-fold CV during the classification. The application of CV also ensures that the results are robust and therefore the proposed system can be used in some practical setup for treatment, monitoring or diagnosis. The practical setup may help the clinicians and medical professionals in early diagnosis. This may enhance the level of health care of patients. However, before using the model in a practical setup, it is strongly recommended that the performance of the proposed system be judged using some other dataset of large dimension. In order to justify the effectiveness of the proposed system, one needs to evaluate the performance using some other data set of larger size. In this study, we have used features extracted from DPB optimal three-band FB, instead of using conventional two-band FBS. We found that the performance of the features extracted from TPOWFB is better than the previously employed two-band FBs in classifying normal and alcoholic EEG signals. This establishes the superiority of three-band FBs over two-band FBs in alcoholism identification. In this study, we have used log-energy of SBs that are obtained using TBOWFB. It will be an interesting study to check the performance of the DPB optimal TBOWFB taking non-linear features [5] as discriminating features in an alcoholic detection system. It may also be of interest to develop an index [2, 4] to measure alcoholism taking the features obtained from SBs of the optimal TBOWFB.

The automated diagnosis system is a cost-effective and non-invasive technique. Hence, it can be easily employed in all the hospitals and remote villages also. The proposed computer aided system enables medical professionals to detect alcoholism in a subject who does not show symptoms of an alcohol abuse, thereby bringing a cost benefit for the relevant health services. Our study shows that the optimal TBOWFB as applied to EEG signals are found to be an effective automatic identification scheme for alcoholic and normal subjects. In future, the method can used to detect the different stages of alcoholism using EEG signals. Our technique can be used to reduce road accidents by finding the drivers who drive under the influence of alcohol. Also, this algorithm can be extended to detect other neural abnormalities like epilepsy, autism, dementia, down syndrome, etc. using EEG signals.

## References


1. Acharya UR, Bhat S, Adeli H, Adeli A et al (2014) Computer-aided diagnosis of alcoholism-related eeg signals. Epilepsy Behav 41:257–263
2. Acharya UR, Mookiah MRK, Koh JE, Tan JH, Bhandary SV, Rao AK, Hagiwara Y, Chua CK, Laude A (2017) Automated diabetic macular edema (dme) grading system using dwt, dct features and maculopathy index. Comput Biol Med 84:59–68
3. Acharya UR, Sree SV, Chattopadhyay S, Suri JS (2012) Automated diagnosis of normal and alcoholic eeg signals. Int J Neural Syst 22(3):1250,011
4. Acharya UR, Sree SV, Krishnan MMR, Molinari F, Saba L, Ho SYS, Ahuja AT, Ho SC, Nicolaides A, Suri JS (2012) Atherosclerotic risk stratification strategy for carotid arteries using texture-based features. Ultrasound Med Biol 38(6):899–915
5. Acharya UR, Sree SV, Swapna G, Martis RJ, Suri JS (2013) Automated EEG analysis of epilepsy: a review. Knowl-Based Syst 45:147–165
6. Bhati D, Sharma M, Pachori RB, Gadre V (2017) Time-frequency localized three-band biorthogonal wavelet filter bank using semidefinite relaxation and nonlinear least squares with epileptic seizure EEG signal classification. Digital Signal Process 62:259–273
7. Bhati D, Sharma M, Pachori RB, Nair SS, Gadre V (2016) Design of time–frequency optimal three-band wavelet filter banks with unit sobolev regularity using frequency domain sampling. Circuits Syst Signal Process 35(12):4501–4531
8. Bhattacharyya A, Sharma M, Pachori RB, Sircar P, Acharya UR (2016) A novel approach for automated detection of focal eeg signals using empirical wavelet transform. Neural Computing and Applications, pp 1–11

9. Boser BE, Guyon IM, Vapnik VN (1992) A training algorithm for optimal margin classifiers. In: Proceedings of the fifth annual workshop on computational learning theory. ACM, pp 144–152
10. Burrus C, Gopinath RA, Guo H (1998) Introduction to wavelets and wavelet transforms: A primer
11. Cherpitel CJ (2009) Alcohol and injuries: emergency department studies in an international perspective. World Health Organization
12. Chui CK, Lian JA (1995) Construction of compactly supported symmetric and antisymmetric orthonormal wavelets with scale= 3. Appl Comput Harmon Anal 2(1):21–51
13. Cortes C, Vapnik V (1995) Support-vector networks . Mach Learn 20(3):273–297
14. Cristianini N, Shawe-Taylor J (2000) An introduction to support vector machines and other kernel-based learning methods. Cambridge University Press
15. Daubechies I (1988) Orthonormal bases of compactly supported wavelets. Commun Pure Appl Math 41(7):909–996
16. Druesne-Pecollo N, Tehard B, Mallet Y, Gerber M, Norat T, Hercberg S, Latino-Martel P (2009) Alcohol and genetic polymorphisms: effect on risk of alcohol-related cancer. Lancet Oncol 10(2):173–180
17. Ehlers CL, Havstad J, Prichard D, Theiler J (1998) Low doses of ethanol reduce evidence for nonlinear structure in brain activity. J Neurosci 18(18):7474–7486
18. Ethem A (2004) Introduction to machine learning (adaptive computation and machine learning). Mass MIT Press, Cambridge
19. Faust O, Acharya R, Allen AR, Lin C (2008) Analysis of eeg signals during epileptic and alcoholic states using ar modeling techniques. IRBM 29(1):44–52
20. Faust O, Yu W, Kadri NA (2013) Computer-based identification of normal and alcoholic eeg signals using wavelet packets and energy measures. J Mech Med Biol 13(3):1350,033
21. Gabor D (1946) Theory of communication. Proc Inst Elec Eng 93(26):429–441
22. Gopinath RA (1993) Wavelets and filter banks-new results and applications. Ph.D. thesis, Rice University
23. Howlett M, Nguyen T, Davis R (2002) A 3-channel biorthogonal filter bank construction based on predict and update lifting steps. Real-Time Imaging and Sensing Group
24. Jayawardena A (2003) 3-band linear phase bi-orthogonal wavelet filter banks. In: Proceedings of the 3rd IEEE international symposium on signal processing and information technology, 2003. ISSPIT 2003. IEEE, pp 46–49
25. Kannathal N, Acharya UR, Lim CM, Sadasivan P (2005) Characterization of eeg comparative study. Comput Methods Prog Biomed 80(1):17–23
26. Kohavi R et al (1995) A study of cross-validation and bootstrap for accuracy estimation and model selection, pp 1137–1145
27. Lin T, Xu S, Shi Q, Hao P (2006) An algebraic construction of orthonormal m-band wavelets with perfect reconstruction. Appl Math Comput 172(2):717–730
28. Mitchell TM, Michell T (1997) Machine learning. McGraw-Hill Series in Computer Science
29. Organization WH et al (2004) Global status report on alcohol 2004
30. Patidar S, Pachori RB, Upadhyay A, Acharya UR (2017) An integrated alcoholic index using tunable-q wavelet transform based features extracted from eeg signals for diagnosis of alcoholism. Appl Soft Comput 50:71–78
31. Peng L, Wang Y (2001) Parameterization and algebraic structure of 3-band orthogonal wavelet systems. Sci China, Ser A Math 44(12):1531–1543
32. Sharma M, Achuth PV, Pachori RB, Gadre V (2017) A parametrization technique to design joint time–frequency optimized discrete-time biorthogonal wavelet bases. Signal Process 135:107–120
33. Sharma M, Bhati D, Pillai S, Pachori RB, Gadre V (2016) Design of time–frequency localized filter banks: transforming non-convex problem into convex via semidefinite relaxation technique. Circuits Syst Signal Process 35(10):3716–3733
34. Sharma M, Dhere A, Pachori RB, Acharya UR (2017) An automatic detection of focal EEG signals using new class of time–frequency localized orthogonal wavelet filter banks. Knowl-Based Syst 118:217–227
35. Sharma M, Dhere A, Pachori RB, Gadre V (2017) Optimal duration-bandwidth localized antisymmetric biorthogonal wavelet filters. Signal Process 134:87–99
36. Sharma M, Gadre V, Porwal S (2014) An eigenfilter-based approach to the design of time-frequency localization optimized two-channel linear phase biorthogonal filter banks. Circuits, Systems, and Signal Processing
37. Sharma M, Kolte R, Patwardhan P, Gadre V (2010) Time-frequency localization optimized biorthogonal wavelets. In: International conference on signal processing and communication (SPCOM), 2010, pp 1–5
38. Sharma M, Pachori RB, Acharya UR (2017) A new approach to characterize epileptic seizures using analytic time-frequency flexible wavelet transform and fractal dimension. Pattern Recognition Letters. https://doi.org/10.1016/j.patrec.2017.03.023. http://www.sciencedirect.com/science/article/pii/S0167865517300995
39. Sharma M, Singh T, Bhati D, Gadre V (2014) Design of two-channel linear phase biorthogonal wavelet filter banks via convex optimization. In: 2014 international conference on signal processing and communications (SPCOM), pp 1–6. https://doi.org/10.1109/SPCOM.2014.6983931
40. Sharma M, Vanmali AV, Gadre V (2013) Wavelets and fractals in earth system sciences, chap. Construction of Wavelets. CRC Press, Taylor and Francis Group
41. Strutz T (2009) Design of three-channel filter banks for lossless image compression. In: 2009 16th IEEE international conference on image processing (ICIP). IEEE, pp 2841–2844
42. Suykens JA, Vandewalle J (1999) Least squares support vector machine classifiers. Neural Process Lett 9(3):293–300
43. Tcheslavski GV, Gonen FF (2012) Alcoholism-related alterations in spectrum, coherence, and phase synchrony of topical electroencephalogram. Comput Biol Med 42(4):394–401
44. Vapnik V (1995) The nature of statistical learning theory. Springer-Verlag, New York
45. Vaidyanathan P (1987) Quadrature mirror filter banks, m-band extensions and perfect-reconstruction techniques. IEEE ASSP Mag 4(3):4–20
46. Vaidyanathan PP (1993) Multirate systems and filter banks. Prentice-Hall signal processing series. N.J. Prentice Hall, Englewood Cliffs
47. Vetterli M (1987) A theory of multirate filter banks. IEEE Trans Acoust Speech Signal Process 35(3):356–372
48. Vetterli M, Herley C (1992) Wavelets and filter banks: theory and design. IEEE Trans Signal Process 40(9):2207–2232
49. Zhao P, Zhao C (2013) Three-channel symmetric tight frame wavelet design method. Inf Technol J 12(4):623
50. Zhu W, Wang X, Ma Y, Rao M, Glimm J, Kovach JS (2003) Detection of cancer-specific markers amid massive mass spectral data. Proc Natl Acad Sci 100(25):14,666–14,671